



HAL
open science

Estimating persistent oil contamination in tropical region using vegetation indices and random forest regression

Guillaume Lassalle, Anthony Crédoz, Rémy Hédacq, Georges Bertoni, Dominique Dubucq, Sophie Fabre, Arnaud Elger

► To cite this version:

Guillaume Lassalle, Anthony Crédoz, Rémy Hédacq, Georges Bertoni, Dominique Dubucq, et al.. Estimating persistent oil contamination in tropical region using vegetation indices and random forest regression. *Ecotoxicology and Environmental Safety*, 2019, 184, pp.109654. 10.1016/j.ecoenv.2019.109654 . hal-02296861

HAL Id: hal-02296861

<https://hal.science/hal-02296861>

Submitted on 25 Sep 2019

HAL is a multi-disciplinary open access archive for the deposit and dissemination of scientific research documents, whether they are published or not. The documents may come from teaching and research institutions in France or abroad, or from public or private research centers.

L'archive ouverte pluridisciplinaire **HAL**, est destinée au dépôt et à la diffusion de documents scientifiques de niveau recherche, publiés ou non, émanant des établissements d'enseignement et de recherche français ou étrangers, des laboratoires publics ou privés.

1 Estimating persistent oil contamination in tropical
2 region using vegetation indices and Random Forest
3 regression

4 *Guillaume Lassalle^{a, b}, Anthony Credo^b, Rémy Hédacq^b, Georges Bertoni^c, Dominique Dubucq^d,*
5 *Sophie Fabre^a, Arnaud Elger^e*

6 AUTHOR ADDRESS

7 ^a Office National d'Études et de Recherches Aérospatiales (ONERA), Toulouse, France

8 ^b TOTAL S.A., Pôle d'Études et de Recherches de Lacq, Lacq, France

9 ^c DynaFor, Université de Toulouse, INRA, Castanet-Tolosan, France

10 ^d TOTAL S.A., Centre Scientifique et Technique Jean-Féger, Pau, France

11 ^e EcoLab, Université de Toulouse, CNRS, INPT, UPS, Toulouse, France

12 *Corresponding author: Guillaume Lassalle, Office National d'Études et de Recherches
13 Aérospatiales, 2 Avenue Edouard Belin, 31055 Toulouse, France; E-mail:
14 guillaume.lassalle@onera.fr

15 Keywords: reflectance spectroscopy, soil contamination, Total Petroleum Hydrocarbons,
16 vegetation indices, Random Forest

17

18 ABSTRACT

19 The persistence of soil contamination after cessation of oil activities remains a major
20 environmental issue in tropical regions. The assessment of the contamination is particularly
21 difficult on vegetated sites, but promising advances in reflectance spectroscopy have recently
22 emerged for this purpose. This study aimed to exploit vegetation reflectance for estimating low
23 concentrations of Total Petroleum Hydrocarbons (TPH) in soils. A greenhouse experiment was
24 carried out for 42 days on *Cenchrus alopecuroides* (L.) under realistic tropical conditions. The
25 species was grown on oil-contaminated mud pit soils from industrial sites, with various
26 concentrations of TPH. After 42 days, a significant decrease in plant growth and leaf chlorophyll
27 and carotenoid contents was observed for plants exposed to 5 to 19 g.kg⁻¹ TPH in comparison to
28 the controls ($p < 0.05$). Conversely, pigment contents were higher for plants exposed to 1 g.kg⁻¹
29 TPH (hormesis phenomenon). These modifications proportionally affected the reflectance of *C.*
30 *alopecuroides* at leaf and plant scales, especially in the visible region around 550 and 700 nm. 33
31 vegetation indices were used for linking the biochemical and spectral responses of the species to
32 oil using elastic net regressions. The established models indicated that chlorophylls a and b and
33 β -carotene were the main pigments involved in the modifications of reflectance ($R^2 > 0.7$). The
34 same indices also succeeded in estimating the concentrations of TPH using random forest
35 regression, at leaf and plant scales (RMSE = 1.46 and 1.63 g.kg⁻¹ and RPD = 5.09 and 4.44,
36 respectively). Four out of the 33 indices contributed the most to the models (>75%). This study
37 opens up encouraging perspectives for monitoring the cessation of oil activities in tropical
38 regions. Further researches will focus on the application of our approach at larger scale, on
39 airborne and satellite imagery.

40 1. Introduction

41 Along with its development during the last century, oil and gas industry has become a major
42 source of contamination in the environment (Barraza et al., 2018; Durango-Cordero et al., 2018;
43 Ogri, 2001; Romero et al., 2017). Crude oil and by-products (e.g. petroleum products,
44 wastewater, oil sludge) are frequently released in soils, following accidental facility failures, bad
45 practices and, more rarely, storm events (Ahmadun et al., 2009; Chang and Lin, 2006; Correa
46 Pabón et al., 2019; Hu et al., 2013). They cause important ecological disturbances, because oil

47 contaminants – especially Total Petroleum Hydrocarbons (TPH) – are highly toxic toward
48 organisms (Bejarano and Michel, 2016; Finer et al., 2008; Merkl et al., 2004). The contamination
49 of soil may persist in brownfields and mud pits after cessation of the oil production activity and
50 affect ecosystems on the long term (Lassalle et al., 2019b, 2019a). The monitoring of oil
51 activities has therefore become a critical environmental issue, and gave rise to an increasing need
52 in reliable and cost-effective methods for assessing soil contamination. For this purpose,
53 reflectance spectroscopy provided promising results when applied to bare soils (Correa Pabón
54 and de Souza Filho, 2016; Scafutto and de Souza Filho, 2016). Its application to multi- and
55 hyperspectral remote sensing imagery makes possible to detect and quantify soil TPH content at
56 large scale using airborne sensors (Correa Pabón et al., 2019; Scafutto et al., 2017). More
57 recently, a new approach has been proposed to extend its use to vegetated areas, where oil cannot
58 be detected directly at the soil surface (Lassalle et al., 2018; Rosso et al., 2005; Sanches et al.,
59 2013a). This approach shows great interest in tropical regions, where vegetation is particularly
60 dense (Achard et al., 2018; Adamu et al., 2018; Arellano et al., 2015).

61 TPH affect vegetation health – especially pigment and water contents – and optical properties
62 in the reflective domain (400 – 2500 nm) (Balliana et al., 2017; Emengini et al., 2013a; Rosso et
63 al., 2005; Tran et al., 2018). By exploiting the reflectance of leaves and canopies at particular
64 wavelengths, it is possible to detect the changes induced by TPH in leaf biochemistry (Gürtler et
65 al., 2018; Lassalle et al., 2018; Sanches et al., 2013a). This approach is however still under
66 development and needs further improvements in order to be used operationally. Methods based
67 on vegetation indices (VI) (i.e. reflectance ratios) have succeeded in distinguishing healthy and
68 oil-exposed vegetation and in discriminating among various types of oil contamination, under
69 controlled and natural conditions (Emengini et al., 2013a; Lassalle et al., 2019b). In recent
70 studies, TPH were accurately detected from satellite images (Arellano et al., 2015), but their
71 quantification remains rarely considered, although it is of great interest for assessing the
72 environmental risks deriving from the contamination.

73 The quantification of TPH remains a major challenge, as it implies tracking little variations in
74 leaf biochemistry from its reflectance. This might be particularly difficult on contaminated
75 brownfields and mud pits, because the established species are particularly tolerant to oil exposure
76 (Credoz et al., 2016; Lassalle et al., 2019b). This difficulty is moreover enhanced when dealing
77 with low TPH concentrations, for two main reasons. In most cases, the lower the concentration,

78 the lower the effects on vegetation health and reflectance (Emengini et al., 2013a; Sanches et al.,
79 2013a). These effects become more difficult to detect below a certain concentration (Lassalle et
80 al., 2019b). Moreover, some species undergo a stimulation of growth under exposure to low oil
81 contamination (Kirk et al., 2002; Lin et al., 2002). It is particularly frequent for tropical species.
82 These phenomena make the quantification of TPH very challenging using vegetation reflectance.

83 Previous studies focusing on heavy metals – which is a very different context of soil
84 contamination – achieved accurate quantification of these compounds by exploiting reflectance
85 data in empirical univariate regression models and in Partial Least Square Regression (PLSR)
86 (Shi et al., 2014b, 2014a). Similar approaches proved efficient for quantifying high levels of
87 TPH contamination (up to 77 g.kg⁻¹) in our previous study (Lassalle et al., 2019a), but became
88 ineffective below a certain concentration (~ 20 g.kg⁻¹). So, to date, there is still no evidence that
89 low levels of TPH can be quantified using vegetation reflectance, especially in tropical region.
90 To achieve this, alternative methods are necessary. Emerging machine learning methods, which
91 proved efficient for solving complex regression problems, could help quantifying low TPH
92 concentrations (Hastie et al., 2017; Breiman, 2001).

93 This study aims to assess the potential and limits of vegetation reflectance for quantifying low
94 TPH concentrations in soils, under controlled conditions. The proposed approach relies on the
95 combination of VI and a machine learning method – namely Random Forest (RF) regression.
96 This method was tested on reflectance measurements performed at various acquisition scales,
97 under realistic tropical conditions.

98

99 2. Materials and Methods

100 2.1. Study site and greenhouse experiment

101 An experiment was carried out for 42 days, for which a realistic case of oil contamination was
102 reproduced under controlled tropical conditions. An industrial vegetated mud pit located in
103 tropical region was identified for this purpose. Residues of oil production have been accumulated
104 on this site resulted in persistent oil contamination in soils. After cessation of the activity, the site
105 has been colonized by herbaceous vegetation, mainly *Cenchrus alopecuroides* (L.). The
106 experiment focused on this species, which proved good indicator of oil contamination in
107 previous studies (Emengini et al., 2013c; Lassalle et al., 2018). To reproduce as faithfully as

108 possible the conditions of the mud pit, the soil was sampled on two locations of the site and used
109 in the experiment. Soil analyses revealed low concentrations of BTEX and Polycyclic Aromatic
110 Hydrocarbons (PAHs) in both samples, and C₅-C₄₀ TPH concentrations of 5 and 21 g.kg⁻¹,
111 respectively. The lower (C₅-C₁₀) and intermediate (C₁₀-C₂₁) hydrocarbon fractions have been
112 partially degraded, so the remaining contamination mostly came from the dense ones (C₂₁-C₄₀
113 hydrocarbons), which are poorly degradable and whose uptake by roots is very limited (Lassalle
114 et al., 2019b). Detailed soil analyses can be found in the Supporting Information section. No
115 substantial change in TPH concentrations was observed for the different treatments at the end of
116 the experiment (data not shown). In addition, an uncontaminated soil with similar texture was
117 sampled on another site and used in the experiment. All the soils were homogenized manually
118 and sieved to 10 mm to remove coarse root residuals.

119 Five treatments were applied to *C. alopecuroides* for the greenhouse experiment, with TPH
120 concentrations ranging from 0 to 19 g.kg⁻¹. For this purpose, the soils sampled on the mud pit
121 and the control site were mixed in varying proportions to obtain five levels of contamination,
122 respectively 0 (control), 1, 5, 13 and 19 g.kg⁻¹ TPH (see Supporting Information). Cultivated
123 young plants were acclimated for 15 days in greenhouse and reached 15-cm height before being
124 transplanted in individual pots filled with a 3-cm layer of clay balls and 3 L of the corresponding
125 treatment soil. For each treatment, 11 replicates were grown for 42 days in May and June at 27°
126 C and 70% hygrometry, with a 12:12 light:dark photoperiod provided by natural and artificial
127 light. N-P-K (6-6-6) fertilization was applied weekly to the plants, which were irrigated to field
128 capacity every day. At the end of the experiment, plant shoots were harvested, oven-dried for 48
129 h at 60° C and then weighed.

130

131 2.2. Biochemical analyses and reflectance acquisitions

132 The biochemical and spectral responses of *C. alopecuroides* to the treatments were measured
133 during the study. For this purpose, we followed the procedure described in Lassalle et al.
134 (2019b). Young leaves were sampled on five different replicates per treatment and served for
135 determining leaf water (LWC) and pigment contents (Arellano et al., 2015; Diepens et al., 2017).
136 Leaf pigment content was quantified by High Pressure Liquid Chromatography (HPLC), and
137 included chlorophylls a and b and various carotenoids, such as β-carotene, lutein, antheraxanthin,
138 violaxanthin and zeaxanthin (Barlow et al., 1996). Differences among the treatments were

139 analyzed through ANOVA and Tukey post-hoc tests. In addition, the spectral reflectance of the
140 same sampled leaves was measured following the protocol described below, and linked to
141 biochemical analyses (see section 2.3). This procedure was carried out after 21 and 42 day of
142 experiment. No leaf was sampled before in order to avoid influencing plant growth during early
143 stages.

144 Reflectance measurements were also performed directly on the plants (i.e. without picking
145 leaves) at day 0, 21 and 42, using an ASD FieldSpec 4 Hi-Res spectroradiometer (Malvern
146 Panalytical, Malvern, UK). Data were acquired in radiance in the reflective domain (400 – 2400
147 nm) and converted to reflectance using a white reference calibration panel (Spectralon,
148 Labsphere Inc., North Sutton, USA) (Milton, 1987). For each treatment, three leaves per
149 replicate were measured at random (n = 165 spectra per date) using a leaf-clip with an internal
150 light source (10 measurements averaged per leaf). Additional measurements were conducted at
151 plant scale, by placing a 10°-FOV fore-optic above the pots to obtain a 5-cm wide acquisition
152 footprint (10 measurements averaged per plant). These measurements were performed on each
153 replicate (n = 55 spectra per date) under natural light between 11.30 am and 1.30 pm, under clear
154 sky. The reflectance data from the 1350 – 1450 and 1800 – 1950 nm ranges were not conserved,
155 because of low atmospheric transmission at plant scale. A Savitzky-Golay smoothing filter was
156 then applied at the remaining wavelengths, improving the signal-to-noise ratio (Savitzky and
157 Golay, 1964).

158

159 2.3. Vegetation indices

160 In this study, 33 VI were computed and used in two ways. They are listed in the Supporting
161 Information section. These indices have been specifically exploited for detecting oil-induced
162 changes in leaf biochemistry in our previous study, so here they were tested for quantifying TPH
163 (Lassalle et al. 2019b). Most of them exploited reflectance in the visible (VIS) region (450 – 700
164 nm), which is the most important spectrum region for assessing oil contamination. It has been
165 shown that under exposure to oil, changes in the values of a single vegetation index result from
166 the alteration of several inter-correlated pigments that share common light absorption features
167 (e.g. chlorophylls and carotenoids). Consequently, the pigments to which an index has been
168 initially linked in the literature may differ from those involved in the response to oil exposure.
169 So, it is necessary to identify which pigments contribute the most to index changes, in order to

170 understand how vegetation reflectance is affected by oil. For this purpose, the 33 indices were
171 first computed from the reflectance data of leaves sampled for biochemical analyses, and each of
172 them was linked to leaf pigment and water contents using Elastic net (ENET) multiple regression
173 (Zou and Hastie, 2005), as described in Lassalle et al. (2019b). ENET is a penalized least
174 squared regression method that allows selecting predictors under multicollinearity.
175 Multicollinearity appears when predictors – in our case, leaf pigment contents – are linear
176 combination of each other, and results in confusions when selecting those contributing the most
177 to the target variable (i.e. VI) (Belsley et al., 1980; Dormann et al., 2013). ENET regression
178 prevents from such consequences and has already proved efficient for identifying biochemical
179 parameters involved in reflectance changes under exposure to contaminants (Lassalle et al.,
180 2019b). For each VI, the best predictors were retained and the R^2 of the model was calculated.

181 In a second time, the same 33 indices were computed from the reflectance data acquired at leaf
182 and plant scales and used for predicting TPH concentrations using RF regression (Breiman,
183 2001). RF is an ensemble method that builds and average a lot of independent decision trees to
184 model the relationship between predictors (i.e. the 33 VI) and a response variable – here, TPH
185 concentration (Hastie et al., 2017; Hutengs and Vohland, 2016; Mutanga et al., 2012). Each tree
186 is constructed from a set of decision rules that results from the recursive fragmentation of the
187 original space into successively smaller sub-regions. To define these sub-regions, binary splits
188 are applied independently to each vegetation index. A simple model is then adjusted between VI
189 and TPH concentrations with respect to the splits, and those minimizing the mean squared error
190 between the measured and predicted concentrations are retained. The succession of the selected
191 index splits represents the branches of the decision tree, in such a way that each set of decision
192 rules leads to an estimation of TPH concentration (see Hutengs & Vohland (2016) for a complete
193 description). RF accounts for non-linear relationships between the predictors and the response
194 variable – which can occur for low concentrations of contaminants, so it was of great interest in
195 our case. Moreover, RF informs on the relative contribution of VI to the quantification of TPH
196 (Breiman, 2001; Grömping, 2009), which is essential for operational applications of the method.
197 The RF regression was fitted to half of the data (50% training set) and tested on the remaining
198 part (50% test set), at leaf and plant scales separately (Lassalle et al., 2019b, 2019a). For this
199 purpose, we used the data from day 42, because no difference among the treatments was
200 observed on the previous dates, so no quantification of TPH was possible (see section 3.1). The

201 predictions of TPH made on the test set were compared to those from initial soil analyses based
202 on the R^2 , the Root Mean Squared Error (RMSE) and the Residual Predictive Deviation (RPD)
203 (Shi et al., 2014). The RPD denotes the ratio of the standard deviation of the measured TPH
204 concentrations to the RMSE calculated between the measured and predicted concentrations.

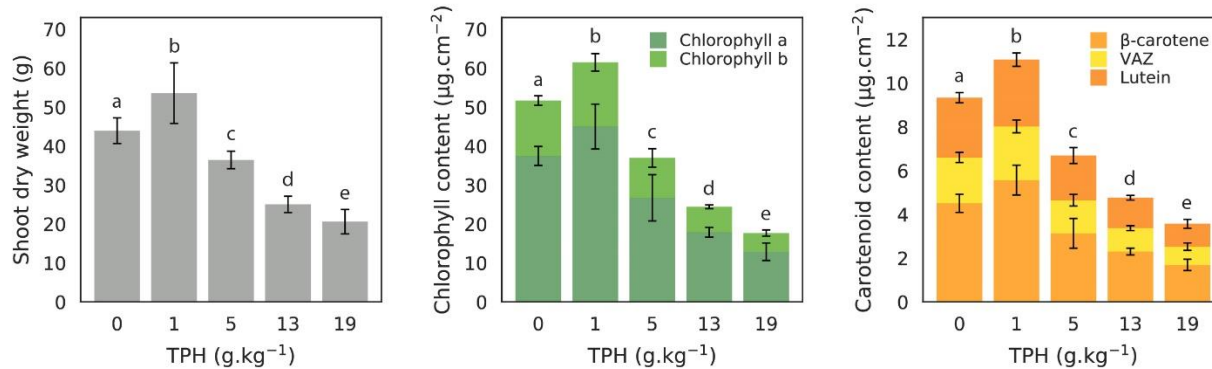
205

206 3. Results and discussion

207 3.1. Biochemical and spectral responses to oil contamination

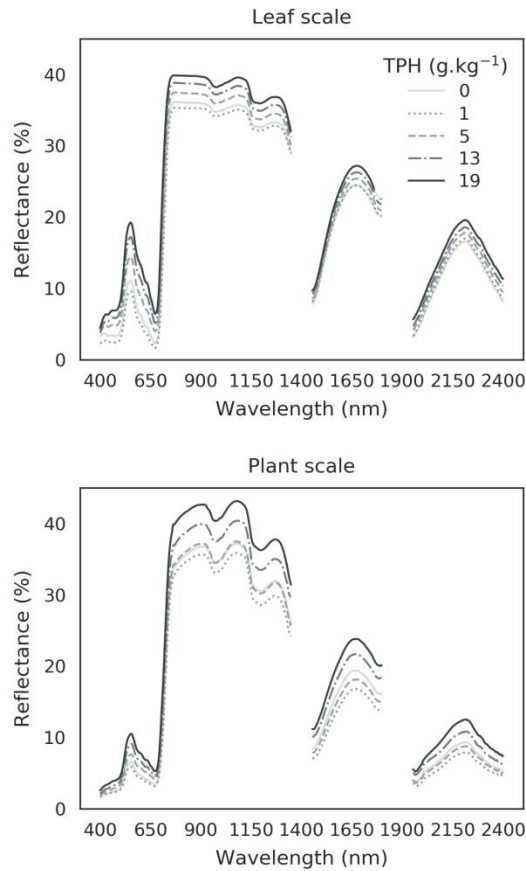
208 As expected, *C. alopecuroides* was highly tolerant to oil, as none of the plants from the
209 contaminated treatments died during the experiment. This observation is consistent with previous
210 studies carried out on the same species with various types of oil contamination (engine oil and oil
211 and gas waste mud) (Emengini et al., 2013c; Lassalle et al., 2018). No visible stress symptom
212 was observed on any of the replicates before the last stages of the experiment (35 – 42 days), so
213 no difference in leaf pigment contents and in leaf and plant reflectance was observed among the
214 treatments on the previous dates (0 and 21 days, data not shown). On day 42, leaf discoloration
215 was observed for the individuals exposed to 5 g.kg⁻¹ TPH or more, expressing a significant
216 decrease in leaf chlorophyll and carotenoid contents when compared to the control ($p < 0.05$)
217 (**Fig. 1**). Plant growth was also significantly affected on this date. The alterations in pigment
218 contents induced an increase of reflectance by 5 to 10% in the VIS region, especially around 550
219 and 700 nm (**Fig. 2**). Other regions of the spectrum were also affected in the same way by
220 contamination. This response was more pronounced at leaf scale, because plant reflectance is
221 also influenced by plant architecture, background soil and illuminating and viewing geometry
222 (Asner, 1997; Sanches et al., 2013a). As suggested in previous works (Emengini et al., 2013c;
223 Lassalle et al., 2018), the late response of *C. alopecuroides* to oil highlights its interest for
224 monitoring long-term contaminated sites, especially brownfields and mud pits remaining after
225 cessation of oil and gas activities.

226



227
 228 Figure 1. Shoot dry weight and leaf chlorophyll and carotenoid contents (mean \pm SD; n = 11 and
 229 5 samples per treatment, respectively) of *C. alopecuroides* after 42 days of exposure to various
 230 levels of Total Petroleum Hydrocarbons (TPH). Significant differences among the treatments are
 231 denoted by different lowercase letters (ANOVA and Tukey post-hoc tests, $p < 0.05$). (VAZ:
 232 Violaxanthin + Antheraxanthin + Zeaxanthin.)

233
 234 Alterations in leaf biochemistry and optical properties are very common for vegetation
 235 exposed to contaminants (Balliana et al., 2017; Lassalle et al., 2019b; Rosso et al., 2005; Sanches
 236 et al., 2013a). They depend on multiple factors, especially the species, the contamination type
 237 and concentration and the time of exposure, and have been previously observed on *C.*
 238 *alopecuroides* and other tropical species (Arellano et al., 2017b; Emengini et al., 2013c; Lassalle
 239 et al., 2017). In the case of oil, these alterations result from the reduction of water and nutrient
 240 availability in soils and uptake capacities of roots (Athar et al., 2016; Balasubramaniam and
 241 Harvey, 2014; Nie et al., 2011). Additional effects may come from the accumulation of
 242 hydrocarbons in tissues (Baruah et al., 2014), but they mostly involve low-carbon TPH, so they
 243 are unlikely to explain the responses observed in our experiment. The amplitude of these
 244 biochemical and spectral responses was determined by the level of contamination, which
 245 confirmed previous results obtained for higher levels of oil (Emengini et al., 2013c; Sanches et
 246 al., 2013a). The more the TPH, the lower the leaf pigment contents and the higher the reflectance
 247 (**Fig. 2**). Consequently, leaf chlorophyll content fell to $17.7 (\pm 3.0) \mu\text{g}\cdot\text{cm}^{-2}$ under exposure to 19
 248 $\text{g}\cdot\text{kg}^{-1}$ TPH, while it reached $51.7 (\pm 3.5) \mu\text{g}\cdot\text{cm}^{-2}$ for control at the end of the experiment (**Fig.**
 249 **1**). A similar trend was observed on carotenoids, and suggested being able to discriminate among
 250 the different levels of contamination using reflectance data.



252

253 Figure 2. Mean reflectance of *C. alopecuroides* in the reflective domain after 42 days of
 254 exposure to various levels of Total Petroleum Hydrocarbons (TPH), at leaf and plant scales.

255 Reflectance data from the 1350–1450 and 1800–1950 intervals were removed, because of low
 256 atmospheric transmission at plant scale. (The legend is common to both figures.)

257

258 In contrast to the other treatments, a stimulating effect was observed for plants exposed to 1
 259 g.kg^{-1} TPH. Shoot dry weight and leaf chlorophyll and carotenoid contents were significantly
 260 higher for this treatment than those of the control ($p < 0.05$), and reflectance was slightly lower
 261 at leaf and plant scales. This particular response – called hormesis – has already been observed
 262 on the growth of other oil-exposed species in previous studies (Kirk et al., 2002; Lin et al., 2002;
 263 Salanitro et al., 1997). However, its causes remain poorly documented. To our knowledge, this
 264 study is the first to bring evidence of this phenomenon using reflectance measurements. Previous
 265 experiments aimed to simulate accidental oil spills (e.g. pipeline leakage), by applying high

266 doses of oil – mainly diesel or engine oil – to crop species, which are particularly sensitive to
267 such contamination (Emengini et al., 2013a; Gürtler et al., 2018; Sanches et al., 2013a).
268 Consequently, strong alterations in leaf biochemistry and reflectance have been observed
269 regardless of the contamination level, so no hormesis has been noticed. The responses of *C.*
270 *alopecuroides* observed in our study substantially differed, because we focused on a totally
271 different context. When oil contamination persists in industrial brownfield and mud pit soils –
272 such as that reproduced in our experiment, the most phytotoxic fractions of petroleum
273 hydrocarbons (e.g. BTEX, PAH) are almost absent from the mixture. The effects on oil-tolerant
274 established vegetation are therefore much less pronounced than those observed for other types of
275 oil contamination with high proportion of these compounds (e.g. crude oil, diesel, gasoline),
276 especially at low concentration (Lassalle et al., 2019b). Here, PAHs and BTEX were found
277 below the detection limits (0.02 and 0.05 mg.kg⁻¹, respectively) at 1 g.kg⁻¹ of TPH and in the
278 control soil, so they did not affect the plants negatively. Conversely, these compounds are likely
279 to induce positive effects at very low concentration (Maliszewska-Kordybach and Smreczak,
280 2000), but they cannot be the only contaminants responsible for the differences observed
281 between the two treatments. Some other hydrocarbon fractions – which were absent from the
282 control soil – enhance the availability of nutrients and organic matter for plants by stimulating
283 microorganisms (Li et al., 1990). Therefore, the very low concentrations of PAHs and BTEX
284 combined to those of other hydrocarbon fractions might have induced the hormetic effect
285 observed in this study.

286

287 3.2. Vegetation indices

288 3.2.1. Elastic net regressions

289 The VI succeeded in linking the biochemical and spectral responses of *C. alopecuroides* to oil
290 contamination. 20 out of the 33 indices tested were strongly correlated to leaf pigment or water
291 content ($R^2 \geq 0.7$) (**Tab. 1**). For most of them, at least three contributing pigments were
292 identified, the others having not being retained by the ENET regression. Chlorophylls and β -
293 carotene were often the most contributing ones, and provided some of the best models ($R^2 \geq 0.8$)
294 when used together (i.e. without addition of other carotenoids). Therefore, these pigments
295 explained most of the modifications in reflectance observed among the treatments in the VIS

296 region. Other carotenoid pigments – especially lutein and violaxanthin – were frequently retained
297 in the models (e.g. GM2 and PSSRb indices), thus confirming previous results obtained on
298 another oil-tolerant species (Lassalle et al., 2019b). These pigment are usually of less
299 contribution to leaf optical properties, because of the masking effect of chlorophylls, which are
300 present at higher concentrations in leaves and share common light absorption features (Ferret et
301 al., 2008; Zhang et al., 2017). Our study shows that they also contribute to the spectral response
302 of vegetation to oil contamination.

303

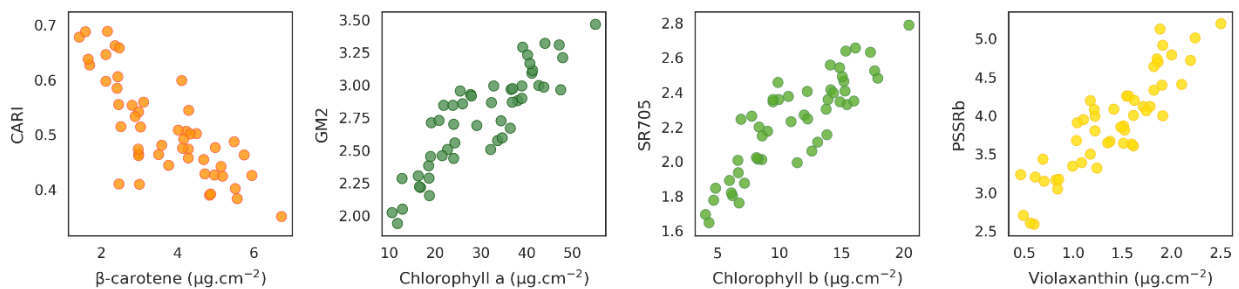
304 Table 1. Results of the elastic net regressions performed on the 33 vegetation indices. For each
 305 index, the R^2 of the model is presented, along with the contributing set of biochemical
 306 parameters (in order of importance). (Chl a: Chlorophyll a, Chl b: Chlorophyll b, B-car: β -
 307 carotene, Lut: Lutein, Ant: Antheraxanthin, Vio: Violaxanthin, Zea: Zeaxanthin, LWC: Leaf
 308 Water Content.)

Index	R^2	Pigments
CARI	0.76	B-car, Chl b
CCI	0.73	B-car, Chl b, Chl a
CTR1	0.24	Vio, B-car, Chl b, Lut, Ant, Zea, Chl a
CTR2	0.81	Chl a, Chl b
GM1	0.84	B-car, Chl b, Chl a
GM2	0.87	Chl a, Chl b, B-car, Lut
LI1	0.65	Chl a, Chl b
LI2	0.18	Chl a
LI3	0.42	Vio, Lut, Ant, Zea, B-car, Chl b, Chl a
mCARI1	0.43	Ant, B-car, Lut, Chl b, Zea, Chl a
mCARI2	0.12	Chl a
mSR705	0.72	Chl a
MTCI	0.84	Chl a, Chl b
ND705	0.82	B-car, Chl b, Chl a
PRI1	0.54	B-car, Vio, Chl b, Zea, Ant, Chl a, Lut
PRI2	0.67	Chl b, Chl a
PRI3	0.63	Chl b, Chl a, Lut
PSRI	0.43	B-car, Chl b, Lut, Ant, Zea, Chl a
PSSRa	0.72	Chl a
PSSRb	0.88	Chl a, Chl b, Lut, B-car, Vio
PSSRc	0.83	Chl a
SIPI1	0.71	Chl a, Chl b
SIPI2	0.81	Chl a, Chl b
SIPI3	0.73	Chl a, Chl b
SR705	0.83	B-car, Chl b, Chl a
TCARI	0.68	B-car, Chl b, Chl a
TCARI_OSAVI	0.75	B-car, Chl b, Chl a
VOG1	0.75	B-car, Chl b, Chl a
VOG2	0.7	B-car, Chl b, Chl a
VOG3	0.71	B-car, Chl b, Vio, Chl a
DWSI	0.82	LWC

309
 310
 311 The close relationship between some indices and contributing pigments are illustrated in
 312 Figure 3. As observed, these indices exhibited strong link with single pigment content. ENET
 313 regression allowed identifying those contributing the most to index changes, in order of

314 importance. These results confirmed the interest of combining pigment contents into multiple
 315 models for better understanding the effects induced by oil contamination on vegetation
 316 reflectance (Lassalle et al., 2019b). Most of the indices exploited reflectance around 550 and 700
 317 nm, which was particularly affected by oil (**Fig. 2**), so they were particularly adapted to our
 318 context of study. The same wavelengths also proved efficient for assessing soil contaminated by
 319 oil and by-products in other situations (oil extraction, pipeline leakages, etc.). Zhu et al. (2014)
 320 exploited reflectance at 700 nm for distinguishing among various levels of alteration in pigment
 321 contents induced by phenanthrene contamination on *Suaeda salsa*. Likewise, Sanches et al.
 322 (Sanches et al., 2013b) used the same spectrum region for assessing the effects of oil leakages on
 323 crops species. One of the main advantages of VI relies on their robustness. Some of them remain
 324 only little affected by bare soil and plant architecture, so they can be applied for tracking subtle
 325 alterations in leaf pigment contents induced by oil at different acquisition scales (e.g. leaf, plant
 326 and canopy) (Blackburn, 1998; Dash and Curran, 2007). For example, the same 33 indices
 327 succeeded in discriminating among various types of oil contamination from leaf to canopy scales
 328 in previous study (Lassalle et al., 2019b). Here, they were suitable for estimating TPH
 329 concentrations in soils.

330



331

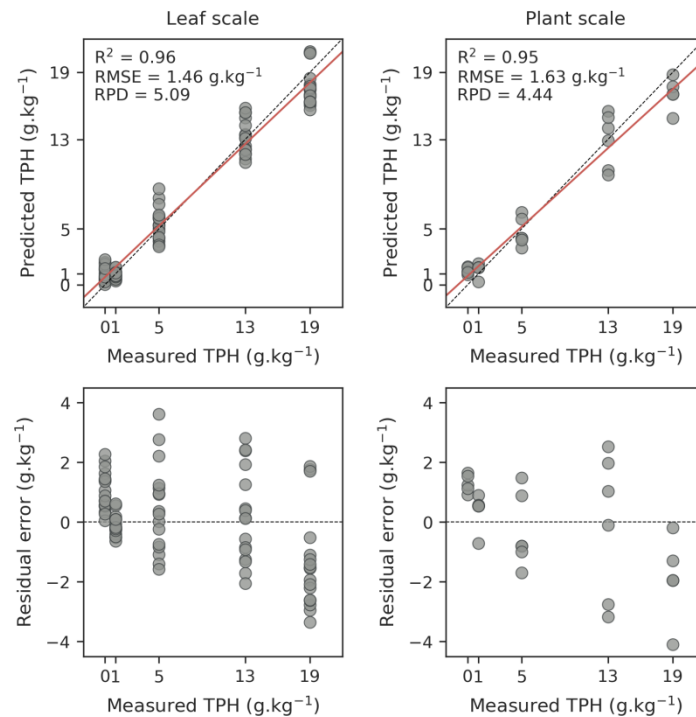
332 Figure 3. Relationship between vegetation indices and leaf pigment contents. Figures include
 333 data from leaves sampled on all the treatments, after 21 and 42 days of experiment (n = 50).

334

335 3.2.2. Random Forest regressions

336 RF regressions performed using the 33 VI provided accurate predictions of TPH
 337 concentrations on the test set, at leaf and plant scales. These results are presented in Figure 4.
 338 High R² values – respectively 0.96 and 0.95 at leaf and plant scales – indicated strong correlation
 339 between the measured and predicted concentrations on the test sets. Predictions of TPH were

340 very close to the true concentrations, as indicated by the low RMSE values obtained at both
 341 scales. This accuracy was confirmed by RPD values greater than 4.4. RPD provides a better
 342 interpretation of predictions, because it compares the RMSE to the variability in the true TPH
 343 concentrations. RPD values above 2 or 3 are usually needed for considering the models reliable
 344 for use. The 33-VI based RF models were therefore particularly adapted for estimating TPH in
 345 our study. The analysis of residuals revealed that the highest level of contamination (19 g.kg⁻¹)
 346 was the most difficult to predict, as it was almost systematically underestimated (**Fig. 4**). This
 347 may be caused by saturation in the spectral response of *C. alopecuroides* to this type of oil
 348 contamination, as described for other species in previous study. Confusions also arose at the
 349 lowest concentrations (0 – 1 g.kg⁻¹). They highlighted the difficulty to detect the hormesis
 350 phenomenon using reflectance data, for which only little differences were observed among the
 351 two treatments (**Fig. 2**). These results thus helped identifying the detection limit of our approach.
 352



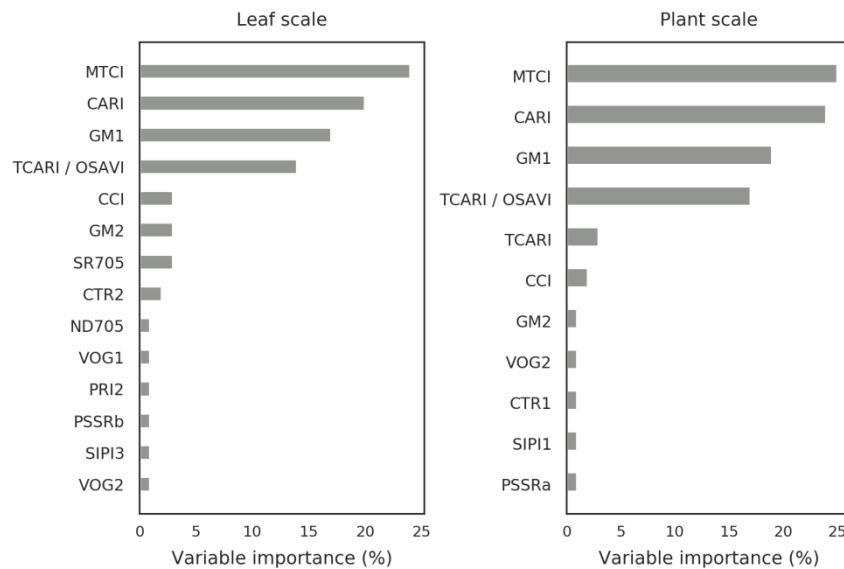
353
 354 Figure 4. Comparison between the measured and predicted concentrations of Total Petroleum
 355 Hydrocarbons (TPH) using the 33 vegetation indices and the random forest regression on the test
 356 set, at leaf and plant scales (top figures), and residuals of the predictions (bottom figures).

357

358 The relative contribution of VI to the RF models was consistent from leaf to plant scales. Four
359 out of the 33 indices contributed the most to TPH predictions ($> 75\%$, **Fig. 5**). These indices
360 were among those closely linked to leaf pigment contents ($R^2 > 0.7$, **Tab. 1**), and more precisely
361 chlorophylls and β -carotene. They exploit reflectance around 550 and 700 nm, but also 670 –
362 680 and 750 nm, which helped enhancing the differences among the treatments. Only few
363 wavelengths are therefore necessary for estimating TPH accurately using reflectance
364 spectroscopy. Conversely, the other indices remained of little contribution to the models ($< 5\%$
365 each), especially those linked to additional carotenoids (e.g. lutein, violaxanthin), because they
366 brought redundant information.

367 The consistence of the results between acquisition scales opens up promising perspectives for
368 operational applications of our approach under natural conditions. Some of the main indices –
369 especially the MTCI and TCARI / OSAVI – have been originally designed for imagery
370 application purposes (Dash and Curran, 2007; Haboudane et al., 2002), and proved efficient for
371 detecting – but not for quantifying – oil contamination in tropical regions. For example, Arellano
372 et al. (2015) used the MTCI index to discriminate among control and oil-contaminated sites in
373 the Amazon forest using hyperspectral satellite images. However, the application of these indices
374 for estimating the level of contamination remained unexplored until now. This study was a first
375 attempt in that direction, but further researches are needed to assess the reliability of our
376 approach under natural conditions, using field measurements, and in the long term using multi-
377 and hyperspectral imagery. High to very high spatial resolution might help achieving this,
378 because the contamination can occur on a few square meters and be therefore difficult to detect
379 using medium to low spatial resolution imagery (Adamu et al., 2018; Arellano et al., 2015). As
380 discussed in section 3.1, the case of persistent low contamination in brownfields and mud pits
381 makes the estimation of TPH very challenging, because of the composition of the contamination
382 and the tolerance of the species. Under natural conditions, additional difficulties should be
383 considered before application of our approach. Vegetation established on brownfields and mud
384 pits is exposed to a multitude of environmental factors that affect its health and reflectance (e.g.
385 drought, waterlogging), especially in the tropical regions with marked seasonality (Adamu et al.,
386 2016; Smith et al., 2004). These factors might overlap with the effects induced by TPH, making
387 their estimation more difficult. Thanks to recent advances, it seems however possible to
388 discriminate among oil and other stressors using reflectance spectroscopy (Emengini et al.,

389 2013b; Lassalle et al., 2019b, 2018). Because of the selective growing conditions imposed, only
 390 few species are generally established on soils with oil (Noomen et al., 2012), as observed on our
 391 study site. This makes the estimation of TPH feasible, provided that these species are oil-
 392 sensitive. Species richness is however very high in some tropical regions subject to oil
 393 contamination (Arellano et al., 2017a, 2017b). Such diversity in plant species means important
 394 differences in sensitivity to oil among them. Some species are totally tolerant to oil, whereas
 395 others are affected even at very low concentration. This makes the estimation of TPH more
 396 difficult, so it is necessary to identify the most suitable species before, as we did under controlled
 397 conditions.
 398



399
 400 Figure 5. Relative contribution of the vegetation indices to the estimation of Total Petroleum
 401 Hydrocarbons (TPH) using random forest regression, at leaf and plant scales. Only indices with
 402 non-zero contribution are displayed.

403
 404 4. Conclusion

405 This study aimed to quantify low TPH concentrations in soils using *C. alopecuroides*
 406 reflectance under controlled tropical conditions. Modifications in leaf biochemistry appeared
 407 after a long-term exposure, depending on the level of contamination. Pigment contents were
 408 reduced for TPH concentrations of 5 g.kg⁻¹ and above, whereas they increased at lower

409 concentration when compared to control. These modifications were linked to the reflectance data
410 through VI, which brought evidence of the implication of chlorophylls and various carotenoids in
411 the spectral response of the species to oil. The same indices succeeded in predicting TPH
412 concentrations with good accuracy using RF regressions, at leaf and plant scales. Four out of the
413 33 indices tested were almost sufficient to achieve these predictions. This study emphasizes the
414 potential of reflectance spectroscopy for quantifying oil contamination in tropical regions with
415 dense vegetation. More specifically, the long-term response of *C. alopecuroides* to oil highlights
416 its interest for assessing persistent contamination, for example after cessation of the oil
417 production activity. Although our approach is at early stage and needs further improvements, we
418 are convinced that it could soon result in imagery applications. The emergence of new satellite-
419 and UAV-embedded hyperspectral sensors is sparking a growing interest by oil and gas
420 companies, because they could help assessing oil contamination locally or at large scale. Our
421 study under controlled conditions was the first necessary step prior to such applications. In its
422 continuity, our upcoming research will focus on the adaptation of the approach to hyperspectral
423 imagery with high spatial resolution, and its assessment in tropical region with heavy past oil and
424 gas production activities.

425

426 Acknowledgements

427 This interdisciplinary work was achieved in the frame of the NAOMI R&D project between
428 TOTAL and the ONERA, with the support of Ecolab and Dynafor research units of Toulouse.
429 The authors gratefully acknowledge E. Buffan-Dubau, D. Lambrigot and O. Berseille for their
430 assistance in pigment analysis.

431 Declarations of interest: None.

432 Funding: Financial support of this work was provided by TOTAL.

433 References

434

435 Achard, V., Fabre, S., Alakian, A., Dubucq, D., Déliot, P., 2018. Direct or indirect on-shore
436 hydrocarbon detection methods applied to hyperspectral data in tropical area, in: Michel, U.,
437 Schulz, K. (Eds.), *Earth Resources and Environmental Remote Sensing/GIS Applications*
438 IX. SPIE, p. 22. <https://doi.org/10.1117/12.2325097>

439 Adamu, B., Tansey, K., Ogutu, B., 2018. Remote sensing for detection and monitoring of
440 vegetation affected by oil spills. *Int. J. Remote Sens.* 39, 3628–3645.
441 <https://doi.org/10.1080/01431161.2018.1448483>

442 Adamu, B., Tansey, K., Ogutu, B., 2016. An investigation into the factors influencing the
443 detectability of oil spills using spectral indices in an oil-polluted environment. *Int. J.*
444 *Remote Sens.* 37, 2338–2357. <https://doi.org/10.1080/01431161.2016.1176271>

445 Ahmadun, F.-R., Pendashteh, A., Abdullah, L.C., Awang Biak, D.R., Madaeni, S.S., Abidin,
446 Z.Z., 2009. Review of technologies for oil and gas produced water treatment. *J. Hazard.*
447 *Mater.* 170, 530–551. <https://doi.org/10.1016/j.jhazmat.2009.05.044>

448 Arellano, P., Tansey, K., Balzter, H., Boyd, D.S., 2017a. Field spectroscopy and radiative
449 transfer modelling to assess impacts of petroleum pollution on biophysical and biochemical
450 parameters of the Amazon rainforest. *Environ. Earth Sci.* 76, 1–14.
451 <https://doi.org/10.1007/s12665-017-6536-6>

452 Arellano, P., Tansey, K., Balzter, H., Boyd, D.S., 2015. Detecting the effects of hydrocarbon
453 pollution in the Amazon forest using hyperspectral satellite images. *Environ. Pollut.* 205,
454 225–239. <https://doi.org/10.1016/j.envpol.2015.05.041>

455 Arellano, P., Tansey, K., Balzter, H., Tellkamp, M., 2017b. Plant family-specific impacts of
456 petroleum pollution on biodiversity and leaf chlorophyll content in the Amazon rainforest of
457 Ecuador. *PLoS One* 12. <https://doi.org/10.1371/journal.pone.0169867>

458 Asner, G.P., 1997. Biophysical and Biochemical Sources of Variability in Canopy Reflectance.
459 *Remote Sens. Environ.* 64, 234–253.

460 Athar, H. ur R., Ambreen, S., Javed, M., Hina, M., Rasul, S., Zafar, Z.U., Manzoor, H., Ogbaga,
461 C.C., Afzal, M., Al-Qurainy, F., Ashraf, M., 2016. Influence of sub-lethal crude oil
462 concentration on growth, water relations and photosynthetic capacity of maize (*Zea mays*
463 *L.*) plants. *Environ. Sci. Pollut. Res.* 23, 18320–18331. <https://doi.org/10.1007/s11356-016-6976-7>

465 Balasubramaniyam, A., Harvey, P.J., 2014. Scanning electron microscopic investigations of root
466 structural modifications arising from growth in crude oil-contaminated sand. *Environ. Sci.*
467 *Pollut. Res.* 21, 12651–12661. <https://doi.org/10.1007/s11356-014-3138-7>

468 Balliana, A.G., Moura, B.B., Inckot, R.C., Bona, C., 2017. Development of *Canavalia ensiformis*
469 in soil contaminated with diesel oil. *Environ. Sci. Pollut. Res.* 24, 979–986.
470 <https://doi.org/10.1007/s11356-016-7674-1>

- 471 Barlow, R.G., Cummings, D.G., Gibb, S.W., 1996. Improved resolution of mono- and divinyl
472 chlorophylls a and b and zeaxanthin and lutein in phytoplankton extracts using reverse
473 phase C-8 HPLC. *Mar. Ecol. Prog. Ser.* 161, 303–307.
- 474 Barraza, F., Maurice, L., Uzu, G., Becerra, S., López, F., Ochoa-Herrera, V., Ruales, J., Schreck,
475 E., 2018. Distribution, contents and health risk assessment of metal(loid)s in small-scale
476 farms in the Ecuadorian Amazon: An insight into impacts of oil activities. *Sci. Total*
477 *Environ.* 622–623, 106–120. <https://doi.org/10.1016/j.scitotenv.2017.11.246>
- 478 Baruah, P., Saikia, R.R., Baruah, P.P., Deka, S., 2014. Effect of crude oil contamination on the
479 chlorophyll content and morpho-anatomy of *Cyperus brevifolius* (Rottb.) Hassk. *Environ.*
480 *Sci. Pollut. Res.* 21, 12530–12538. <https://doi.org/10.1007/s11356-014-3195-y>
- 481 Bejarano, A.C., Michel, J., 2016. Oil spills and their impacts on sand beach invertebrate
482 communities: A literature review. *Environ. Pollut.* 218, 709–722.
483 <https://doi.org/10.1016/j.envpol.2016.07.065>
- 484 Belsley, D.A., Kuh, E., Wemsch, R.E., 1980. Detecting and Assessing Collinearity, in: John
485 Wiley & Sons, I. (Ed.), *Regression Diagnostics: Identifying Influential Data and Sources of*
486 *Collinearity*.
- 487 Blackburn, G.A., 1998. Quantifying chlorophylls and carotenoids at leaf and canopy scales: An
488 evaluation of some hyperspectral approaches. *Remote Sens. Environ.* 66, 273–285.
489 [https://doi.org/10.1016/S0034-4257\(98\)00059-5](https://doi.org/10.1016/S0034-4257(98)00059-5)
- 490 Breiman, L., 2001. Random forests. *Mach. Learn.* 45, 5–32.
491 <https://doi.org/10.1023/A:1010933404324>
- 492 Chang, J.I., Lin, C.C., 2006. A study of storage tank accidents. *J. Loss Prev. Process Ind.* 19, 51–
493 59. <https://doi.org/10.1016/j.jlp.2005.05.015>
- 494 Correa Pabón, R.E., de Souza Filho, C.R., 2016. Spectroscopic characterization of red latosols
495 contaminated by petroleum-hydrocarbon and empirical model to estimate pollutant content
496 and type. *Remote Sens. Environ.* 175, 323–336. <https://doi.org/10.1016/j.rse.2016.01.005>
- 497 Correa Pabón, R.E., de Souza Filho, C.R., Oliveira, W.J. de, 2019. Reflectance and imaging
498 spectroscopy applied to detection of petroleum hydrocarbon pollution in bare soils. *Sci.*
499 *Total Environ.* 649, 1224–1236. <https://doi.org/10.1016/j.scitotenv.2018.08.231>
- 500 Credoz, A., Hédacq, R., Barreau, C., Dubucq, D., 2016. Experimental study of hyperspectral
501 responses of plants grown on mud pit soil, in: *Earth Resources and Environmental Remote*
502 *Sensing/GIS Applications VII*. p. 100051E. <https://doi.org/10.1117/12.2239606>
- 503 Dash, J., Curran, P.J., 2007. Evaluation of the MERIS terrestrial chlorophyll index (MTCI). *Adv.*
504 *Sp. Res.* 39, 100–104. <https://doi.org/10.1016/j.asr.2006.02.034>
- 505 Diepens, N.J., Buffan-Dubau, E., Budzinski, H., Kallerhoff, J., Merlina, G., Silvestre, J., Auby,
506 I., Nathalie Tapie, Elger, A., 2017. Toxicity effects of an environmental realistic herbicide
507 mixture on the seagrass *Zostera noltei*. *Environ. Pollut.* 222, 393–403.
508 <https://doi.org/10.1016/j.envpol.2016.12.021>

- 509 Dormann, C.F., Elith, J., Bacher, S., Buchmann, C., Carl, G., Carré, G., Marquéz, J.R.G.,
510 Gruber, B., Lafourcade, B., Leitão, P.J., Münkemüller, T., McClean, C., Osborne, P.E.,
511 Reineking, B., Schröder, B., Skidmore, A.K., Zurell, D., Lautenbach, S., 2013. Collinearity:
512 a review of methods to deal with it and a simulation study evaluating their performance.
513 *Ecography (Cop.)*. 36, 27–46. <https://doi.org/10.1111/j.1600-0587.2012.07348.x>
- 514 Durango-Cordero, J., Saqalli, M., Laplanche, C., Locquet, M., Elger, A., 2018. Spatial Analysis
515 of Accidental Oil Spills Using Heterogeneous Data: A Case Study from the North-Eastern
516 Ecuadorian Amazon. *Sustainability* 10, 4719. <https://doi.org/10.3390/su10124719>
- 517 Emengini, E.J., Blackburn, G.A., Theobald, J.C., 2013a. Early detection of oil-induced stress in
518 crops using spectral and thermal responses. *J. Appl. Remote Sens.* 7.
519 <https://doi.org/10.1117/1.jrs.7.073596>
- 520 Emengini, E.J., Blackburn, G.A., Theobald, J.C., 2013b. Detection and discrimination of oil and
521 water deficit-induced stress in maize (*Zea mays* L.) using spectral and thermal responses.
522 *IOSR J. Environ. Sci. Toxicol. Food Technol.* 3, 53–57.
- 523 Emengini, E.J., Ezeh, F.C., Chigbu, N., 2013c. Comparative Analysis of Spectral Responses of
524 Varied Plant Species to Oil Stress. *Int. J. Sci. Eng. Res.* 4, 1421–1427.
- 525 Feret, J.B., François, C., Asner, G.P., Gitelson, A.A., Martin, R.E., Bidel, L.P.R., Ustin, S.L., le
526 Maire, G., Jacquemoud, S., 2008. PROSPECT-4 and 5: Advances in the leaf optical
527 properties model separating photosynthetic pigments. *Remote Sens. Environ.* 112, 3030–
528 3043. <https://doi.org/10.1016/j.rse.2008.02.012>
- 529 Finer, M., Jenkins, C.N., Pimm, S.L., Keane, B., Ross, C., 2008. Oil and gas projects in the
530 Western Amazon: Threats to wilderness, biodiversity, and indigenous peoples. *PLoS One* 3.
531 <https://doi.org/10.1371/journal.pone.0002932>
- 532 Grömping, U., 2009. Variable importance assessment in regression: Linear regression versus
533 random forest. *Am. Stat.* 63, 308–319. <https://doi.org/10.1198/tast.2009.08199>
- 534 Gürtler, S., de Souza Filho, C.R., Sanches, I.D., Alves, M.N., Oliveira, W.J., 2018.
535 Determination of changes in leaf and canopy spectra of plants grown in soils contaminated
536 with petroleum hydrocarbons. *ISPRS J. Photogramm. Remote Sens.* 146, 272–288.
537 <https://doi.org/10.1016/j.isprsjprs.2018.09.011>
- 538 Haboudane, D., Miller, J.R., Tremblay, N., Zarco-Tejada, P.J., Dextraze, L., 2002. Integrated
539 narrow-band vegetation indices for prediction of crop chlorophyll content for application to
540 precision agriculture. *Remote Sens. Environ.* 81, 416–426. [https://doi.org/10.1016/S0034-4257\(02\)00018-4](https://doi.org/10.1016/S0034-4257(02)00018-4)
- 542 Hastie, T., Tibshirani, R., Friedman, J., 2017. *The Elements of Statistical Learning The Elements*
543 *of Statistical Learning*.
- 544 Hu, G., Li, J., Zeng, G., 2013. Recent development in the treatment of oily sludge from
545 petroleum industry: A review. *J. Hazard. Mater.* 261, 470–490.
546 <https://doi.org/10.1016/j.jhazmat.2013.07.069>

- 547 Hutengs, C., Vohland, M., 2016. Downscaling land surface temperatures at regional scales with
548 random forest regression. *Remote Sens. Environ.* 178, 127–141.
549 <https://doi.org/10.1016/j.rse.2016.03.006>
- 550 Kirk, J.L., Klironomos, J.N., Lee, H., Trevors, J.T., 2002. Phytotoxicity assay to assess plant
551 species for phytoremediation of petroleum-contaminated soil. *Bioremediat. J.* 6, 57–63.
552 <https://doi.org/10.1080/10889860290777477>
- 553 Lassalle, G., Credo, A., Fabre, S., Elger, A., Hédacq, R., Dubucq, D., 2017. Hyperspectral
554 signature analysis of three plant species to long-term hydrocarbon and heavy metal
555 exposure, in: Michel, U., Schulz, K. (Eds.), *Earth Resources and Environmental Remote*
556 *Sensing/GIS Applications VIII*. SPIE, p. 33. <https://doi.org/10.1117/12.2277709>
- 557 Lassalle, G., Credo, A., Hédacq, R., Fabre, S., Dubucq, D., Elger, A., 2018. Assessing Soil
558 Contamination Due to Oil and Gas Production Using Vegetation Hyperspectral Reflectance.
559 *Environ. Sci. Technol.* 52, 1756–1764. <https://doi.org/10.1021/acs.est.7b04618>
- 560 Lassalle, G., Fabre, S., Credo, A., Hédacq, R., Bertoni, G., Dubucq, D., Elger, A., 2019a.
561 Application of PROSPECT for estimating total petroleum hydrocarbons in contaminated
562 soils from leaf optical properties. *J. Hazard. Mater.* 377, 409–417.
563 <https://doi.org/10.1016/j.jhazmat.2019.05.093>
- 564 Lassalle, G., Fabre, S., Credo, A., Hédacq, R., Borderies, P., Bertoni, G., Erudel, T., Buffan-
565 Dubau, E., Dubucq, D., Elger, A., 2019b. Detection and discrimination of various oil-
566 contaminated soils using vegetation reflectance. *Sci. Total Environ.* 655, 1113–1124.
567 <https://doi.org/10.1016/j.scitotenv.2018.11.314>
- 568 Li, Y., Morris, J.T., Yoch, D.C., 1990. Chronic Low Level Hydrocarbon Amendments Stimulate
569 Plant Growth and Microbial Activity in Salt-Marsh Microcosms. *J. Appl. Ecol.* 27, 159–
570 171. <https://doi.org/10.2307/2403575>
- 571 Lin, Q., Mendelssohn, I.A., Suidan, M.T., Lee, K., Venosa, A.D., 2002. The dose-response
572 relationship between No. 2 fuel oil and the growth of the salt marsh grass, *Spartina*
573 *alterniflora*. *Mar. Pollut. Bull.* 44, 897–902. [https://doi.org/10.1016/S0025-326X\(02\)00118-2](https://doi.org/10.1016/S0025-326X(02)00118-2)
- 574 2
- 575 Maliszewska-Kordybach, B., Smreczak, B., 2000. Ecotoxicological Activity of Soils Polluted
576 with Polycyclic Aromatic Hydrocarbons (PAHs) - Effect on Plants. *Environ. Technol.* 21,
577 1099–1110. <https://doi.org/10.1080/09593330.2000.9618996>
- 578 Merkl, N., Schultze-Kraft, R., Infante, C., 2004. Phytoremediation in the tropics-the effect of
579 crude oil on the growth of tropical plants. *Bioremediat. J.* 8, 177–184.
580 <https://doi.org/10.1080/10889860490887527>
- 581 Milton, E.J., 1987. Principles of field spectroscopy. *Int. J. Remote Sens.* 8, 1807–1827.
582 <https://doi.org/https://doi.org/10.1080/01431168708954818>
- 583 Mutanga, O., Adam, E., Cho, M.A., 2012. High density biomass estimation for wetland
584 vegetation using worldview-2 imagery and random forest regression algorithm. *Int. J. Appl.*

- 585 Earth Obs. Geoinf. 18, 399–406. <https://doi.org/10.1016/j.jag.2012.03.012>
- 586 Nie, M., Lu, M., Yang, Q., Zhang, X., Xiao, M., Jiang, L., Yang, J., Fang, C., Chen, J., Li, B.,
587 2011. Plants' use of different nitrogen forms in response to crude oil contamination 159,
588 157–163. <https://doi.org/10.1016/j.envpol.2010.09.013>
- 589 Noomen, M.F., van der Werff, H.M.A., van der Meer, F.D., 2012. Spectral and spatial indicators
590 of botanical changes caused by long-term hydrocarbon seepage. *Ecol. Inform.* 8, 55–64.
591 <https://doi.org/10.1016/j.ecoinf.2012.01.001>
- 592 Ogrí, O.R., 2001. A review of the Nigerian petroleum industry and the associated environmental
593 problems. *Environmentalist* 21, 11–21.
594 <https://doi.org/https://doi.org/10.1023/A:1010633903226>
- 595 Romero, I.C., Toro-Farmer, G., Diercks, A.R., Schwing, P., Muller-Karger, F., Murawski, S.,
596 Hollander, D.J., 2017. Large-scale deposition of weathered oil in the Gulf of Mexico
597 following a deep-water oil spill. *Environ. Pollut.* 228, 179–189.
598 <https://doi.org/10.1016/j.envpol.2017.05.019>
- 599 Rosso, P.H., Pushnik, J.C., Lay, M., Ustin, S.L., 2005. Reflectance properties and physiological
600 responses of *Salicornia virginica* to heavy metal and petroleum contamination. *Environ.*
601 *Pollut.* 137, 241–252. <https://doi.org/10.1016/j.envpol.2005.02.025>
- 602 Salanitro, J.P., Dorn, P.B., Huesemann, M.H., Moore, K.O., Rhodes, I.A., Rice Jackson, L.M.,
603 Vipond, T.E., Western, M.M., Wisniewski, H.L., 1997. Crude oil hydrocarbon
604 bioremediation and soil ecotoxicity assessment. *Environ. Sci. Technol.* 31, 1769–1776.
605 <https://doi.org/10.1021/es960793i>
- 606 Sanches, I.D., de Souza Filho, C.R., Magalhães, L.A., Quitério, G.C.M., Alves, M.N., Oliveira,
607 W.J., 2013a. Assessing the impact of hydrocarbon leakages on vegetation using reflectance
608 spectroscopy. *ISPRS J. Photogramm. Remote Sens.* 78, 85–101.
609 <https://doi.org/10.1016/j.isprsjprs.2013.01.007>
- 610 Sanches, I.D., Souza Filho, C.R., Magalhães, L.A., Quitério, G.C.M., Alves, M.N., Oliveira,
611 W.J., 2013b. Unravelling remote sensing signatures of plants contaminated with gasoline
612 and diesel: An approach using the red edge spectral feature. *Environ. Pollut.* 174, 16–27.
613 <https://doi.org/10.1016/j.envpol.2012.10.029>
- 614 Savitzky, A., Golay, M.J.E., 1964. Smoothing and Differentiation of Data by Simplified Least
615 Squares Procedures. *Anal. Chem.* 36, 1627–1639. <https://doi.org/10.1021/ac60214a047>
- 616 Scafutto, R.D.M., de Souza Filho, C.R., 2016. Quantitative characterization of crude oils and
617 fuels in mineral substrates using reflectance spectroscopy: Implications for remote sensing.
618 *Int. J. Appl. Earth Obs. Geoinf.* 50, 221–242. <https://doi.org/10.1016/j.jag.2016.03.017>
- 619 Scafutto, R.D.P.M., de Souza Filho, C.R., de Oliveira, W.J., 2017. Hyperspectral remote sensing
620 detection of petroleum hydrocarbons in mixtures with mineral substrates: Implications for
621 onshore exploration and monitoring. *ISPRS J. Photogramm. Remote Sens.* 128, 146–157.
622 <https://doi.org/10.1016/j.isprsjprs.2017.03.009>

- 623 Shi, T., Chen, Y., Liu, Y., Wu, G., 2014a. Visible and near-infrared reflectance spectroscopy —
624 An alternative for monitoring soil contamination by heavy metals. *J. Hazard. Mater.* 265,
625 166–176. <https://doi.org/10.1016/j.jhazmat.2013.11.059>
- 626 Shi, T., Liu, H., Wang, J., Chen, Y., Fei, T., Wu, G., 2014b. Monitoring arsenic contamination in
627 agricultural soils with reflectance spectroscopy of rice plants. *Environ. Sci. Technol.* 48,
628 6264–6272. <https://doi.org/10.1021/es405361n>
- 629 Smith, K.L.L., Steven, M.D.D., Colls, J.J.J., 2004. Use of hyperspectral derivative ratios in the
630 red-edge region to identify plant stress responses to gas leaks. *Remote Sens. Environ.* 92,
631 207–217. <https://doi.org/10.1016/j.rse.2004.06.002>
- 632 Tran, T.H., Gati, E.M., Eshel, A., Winter, G., 2018. Germination , physiological and biochemical
633 responses of acacia seedlings (*Acacia raddiana* and *Acacia tortilis*) to petroleum
634 contaminated soils *. *Environ. Pollut.* 234, 642–655.
635 <https://doi.org/10.1016/j.envpol.2017.11.067>
- 636 Zhang, Y., Huang, J., Wang, F., Blackburn, G.A., Zhang, H.K., Wang, X., Wei, Chuanwen,
637 Zhang, K., Wei, Chen, 2017. An extended PROSPECT : Advance in the leaf optical
638 properties model separating total chlorophylls into chlorophyll a and b. *Sci. Rep.* 7.
639 <https://doi.org/10.1038/s41598-017-06694-y>
- 640 Zou, H., Hastie, T., 2005. Regression and variable selection via the elastic net. *J. R. Stat. Soc.*
641 *Ser. B (Statistical Methodol.* 67, 301–320. [https://doi.org/10.1111/j.1467-](https://doi.org/10.1111/j.1467-9868.2005.00503.x)
642 [9868.2005.00503.x](https://doi.org/10.1111/j.1467-9868.2005.00503.x)
- 643